THE JOURNAL OF PHYSICAL CHEMISTRY B

ARTICLE

pubs.acs.org/JPCB

Protein−Surfactant Interaction: Sodium Dodecyl Sulfate-Induced Unfolding of Ribonuclease A

K. Tejaswi Naidu[†] and N. Prakash Prabhu*

Department of Biotechnology, School of Life Sciences, University of Hyderabad, Hyderabad 500 046, India

Supporting Information

ABSTRACT: Protein−surfactant interaction is widely studied to understand stability and structural changes in proteins. In this Article, we have investigated SDS-induced unfolding of RNase A using absorbance, intrinsic fluorescence of the protein, anisotropy, TNS fluorescence, and near- and far-UV circular dichroism. Unfolding titration curves obtained from the absorbance and fluorescence changes were fitted into a five-state protein unfolding model by assuming formation of three intermediate states. Free energy changes and *m*-values of all four transitions between the native and unfolded state were evaluated. The transitions are categorized into two different regions. Region I, up to 0.5 mM of SDS, involves ionic interaction between the protein and SDS where the secondary and tertiary structure of the protein is altered to a less extent. In region II, hydrophobic interaction dominates and has two distinct transitions. The first transition arises from the aggregation of surfactant molecules around the protein hydrophobic sites. In the following transition, the micelles probably expand more, and a few more hydrophobic sites are occupied by the surfactant. In this region, the tertiary contacts are completely broken, and almost 50% of the secondary structure is lost. The aggregation of SDS around the protein starts well below the CMC. These conformational changes can be explained by the necklace and beads model, and the free energy of formation of such a complex for the RNase A−SDS system is found to be 5.2 (±1.0) kcal mol^{-1}. The probable interaction sites and the mechanism of unfolding have been discussed in detail.

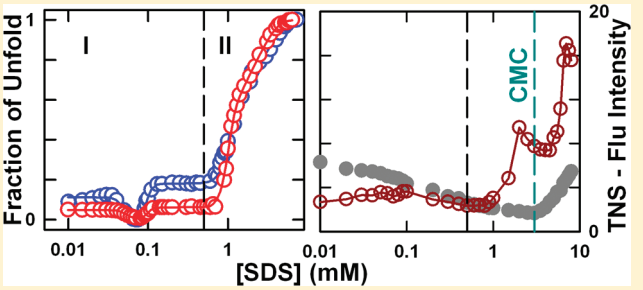

1. INTRODUCTION

Surfactants or surface active agents are amphiphilic molecules that interact at interfaces and reduce the interfacial tension between two phases. Surfactants have a wide range of applications from agriculture and the food industry to cosmetics and the drug industry.[1−3] Despite the fact that surfactants find many uses, their interaction with biological macromolecules is yet to be clearly understood. Interaction of surfactants with biomolecules depends on the charge on the headgroup, length of the hydrophobic tail, and the nature of biomolecule under study.[4] The self-aggregating property of many surfactants that leads to micelle formation makes the system more complex but effective toward various applications. They are regularly used in biochemical laboratories for protein molecular weight determination,[5,6] membrane protein solubilization, and crystallization.[7−9] Therefore, it becomes imperative to follow their effects on biological macromolecules, particularly on proteins.

Protein−surfactant interaction has been studied for a long time.[10−38] It is well-known that surfactants denature proteins well below, almost 1000 times lower than the concentration needed for other chemical denaturants such as urea.[10−24] It encourages scientists to understand the protein unfolding phenomena using surfactants. Proteins interact differently with the monomeric and the micellar forms of surfactants,[24] and they can alter the aggregation properties of surfactants. Further, surfactants are known to induce[25,26] and alter[27] the fibril forming characters of some proteins. Even though a general mechanism for the modulation effect cannot be derived, the experiments clearly show that surfactants can significantly modify the fibrillation kinetics of proteins.

Among the many known surfactants, sodium dodecyl sulfate (SDS) occupies a special place in regular laboratory and industrial use.[1−9] SDS is an anionic surfactant with a long 12-carbon hydrophobic tail and a negatively charged sulfate headgroup. It can induce conformational changes and alter the activities of many proteins.[28−33] Ribonuclease A (Figure 1) is a stable and structurally well-characterized protein.[39] It has served as a very good model to study protein folding right from the Anfinsen's classical experiment.[40,41] However, to our knowledge, specific study on the effect of surfactants on the structure and thermodynamic properties of this protein is very limited.[30−33] Therefore, we attempted to investigate RNase A unfolding by SDS considering the following aspects: (i) It is a basic protein with pI of 9.3.[39] How does addition of an anionic surfactant affect RNase A structure, which has 10 lysine residues on its surface? (ii) What are the similarities and differences in RNase A unfolding as

Received: July 2, 2011
Revised: September 8, 2011
Published: October 20, 2011

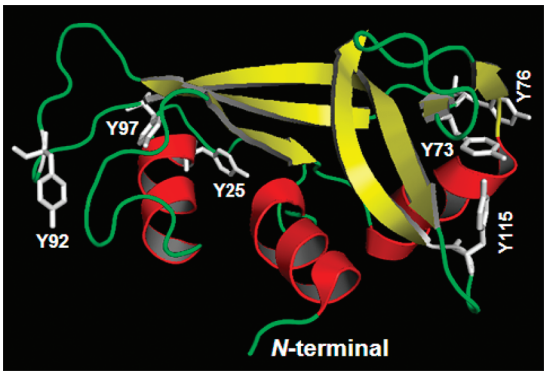

Figure 1. Cartoon diagram of bovine ribonuclease A (PDB id: 1fs3). All six tyrosine residues are labeled and shown in white.

compared to other proteins? (iii) RNase A does not possess any tryptophan residue, but six tyrosine residues. Generally, tyrosine exhibits change in fluorescence intensity but not significant shift in the emission wavelength[42] during chemical and thermal denaturation. Thus, it becomes an interesting question of how tyrosine responds to SDS-induced denaturation. (iv) SDS–protein denaturation reactions are generally illustrated with protein–ligand binding mechanism.[10−14] Only a few attempts have been made to interpret the surfactant-induced unfolding events, following the formalism of protein unfolding with sequential intermediate(s).[15−17] They are nevertheless limited to low surfactant concentrations, which are less from the critical micelle concentration (CMC) of the surfactant and without any identifiable intermediates. Here, we consider the transitions obtained from different probes as a reflection of formation of different conformational states of the protein, before it reaches the unfolded state. It gives a new perspective to understand the interactions with respect to unfolding free energy and *m*-values of transitions between different states involved in the unfolding reaction. Considering the above facts, we monitored the conformational changes of RNase A at different SDS concentrations approximately from 10 μM to 8 mM using different spectroscopic techniques.

2. EXPERIMENTAL METHODS

2.1. Materials. Bovine pancreatic ribonuclease A and *para*-toluidino naphthalene sulfonic acid (TNS) were purchased from Sigma-Aldrich. Sodium dodecyl sulfate, phosphate salts, tyrosine, and safranine O (SO) were obtained from SRL, India.

2.2. Sample Preparation. Different concentrations of SDS stocks were prepared in 20 mM phosphate buffer at pH 7.5 (±0.1). SDS titration of the protein was carried out by preparing aliquots of varying concentrations of SDS from 10 μM to 8 mM using different stock solutions and 20 mM phosphate buffer at pH 7.5 (±0.1). Protein was added either directly into the stock solutions or into the aliquots to obtain the final protein concentration of 12−15 μM. RNase A concentration was calculated from the absorbance value at 278 nm using the molar extinction coefficient value of 9800 M^{-1} cm^{-1}. All of the experiments were carried out at 25 °C.

For TNS fluorescence measurements, equivolume samples with different SDS concentrations were prepared with exactly the same TNS concentration in 20 mM phosphate buffer at pH 7.5. After measuring the emission spectra, protein was equally added to all of the samples in such a way that the increase in the volume of each sample was only 1% and the final protein concentration was ∼12 μM. Spectra obtained were used for further analysis without incorporating any correction factor for the dilution effect.

2.3. Spectroscopic Measurements. Absorbance spectra were recorded from 240 to 300 nm using a Jasco-V 630 spectrophotometer. Protein fluorescence emission spectra were recorded between 290 and 320 nm, after exciting the samples at 280 nm using excitation and emission slit widths of 4 and 6 nm, respectively. Fluorescence anisotropy,[49] r $(=(I_{\parallel} - GI_{\perp})/(I_{\parallel} + 2GI_{\perp}))$ was measured from parallel $(I_{\parallel})$ and perpendicular $(I_{\perp})$ light intensities with *G*-factor correction using the same excitation and emission parameters. To obtain TNS fluorescence intensity changes, samples containing TNS were excited at 320 nm, and emission spectra were measured between 380 and 540 nm. A Horiba Jobin Yvon - fluoromax 3 spectrofluorometer was used to obtain all of the spectra. Ellipticity changes at near- and far-UV were measured in a Jasco J-810 spectropolarimeter. The same set of samples was used to obtain the CD spectra at near and far-UV regions but using 10 and 2 mm path length cuvettes, respectively. Each spectrum was an average of four scans with the scan speed of 20 nm/min.

2.4. Protein Unfolding Model. From the spectral data obtained from different probes, the following five-state model with three sequential intermediates for unfolding (see sections 3.2 and 3.3) was assumed.

$$\mathrm{N} \leftrightarrow \mathrm{I}_1 \leftrightarrow \mathrm{I}_2 \leftrightarrow \mathrm{I}_3 \leftrightarrow \mathrm{U} \quad (1)$$

where N, I_i, and U are native, intermediate, and unfolded states of the protein, respectively.

If the total concentration of different states is [T], then

$$[\mathrm{T}] = [\mathrm{N}] + [\mathrm{I}_1] + [\mathrm{I}_2] + [\mathrm{I}_3] + [\mathrm{U}] \quad (2)$$

The equilibrium constants and the free energy changes between any two states are

$$K_1 = [\mathrm{N}]/[\mathrm{I}_1] \text{ and } \Delta G_1 = -RT \ln K_1$$

$$K_2 = [\mathrm{I}_2]/[\mathrm{I}_3] \text{ and } \Delta G_2 = -RT \ln K_2$$

$$K_3 = [\mathrm{I}_3]/[\mathrm{I}_4] \text{ and } \Delta G_3 = -RT \ln K_3$$

$$K_4 = [\mathrm{I}_4]/[\mathrm{U}] \text{ and } \Delta G_4 = -RT \ln K_4 \quad (3)$$

where R is the gas constant and T is the temperature in kelvin.

For a normalized spectroscopic signal, at any point of denaturant concentration [T] = 1.

The amplitude of the signal is assumed to be a linear combination of contribution from each species:

$$Y = Y_{\mathrm{N}}[\mathrm{N}] + Y_{\mathrm{I1}}[\mathrm{I}_1] + Y_{\mathrm{I2}}[\mathrm{I}_2] + Y_{\mathrm{I3}}[\mathrm{I}_3] + Y_{\mathrm{U}}[\mathrm{U}] \quad (4)$$

where Y_{N}, $Y_{\mathrm{I}i}$, and Y_{U} are specific spectroscopic signals of native, intermediates, and unfolded state, respectively. Next

$$[\mathrm{N}] = 1/(1 + K_1 + K_1K_2 + K_1K_2K_3 + K_1K_2K_3K_4)$$

$$[\mathrm{I}_1] = K_1/(1 + K_1 + K_1K_2 + K_1K_2K_3 + K_1K_2K_3K_4)$$

$$[\mathrm{I}_2] = K_1K_2/(1 + K_1 + K_1K_2 + K_1K_2K_3 + K_1K_2K_3K_4)$$

$$[I_3] = K_1K_2K_3/(1 + K_1 + K_1K_2 + K_1K_2K_3 + K_1K_2K_3K_4)$$

$$[U] = K_1K_2K_3K_4/(1 + K_1 + K_1K_2 + K_1K_2K_3 + K_1K_2K_3K_4) \quad (5)$$

The free energy change of each transition in the absence of denaturant (ΔG_i^0) is given as:

$$\Delta G_i = \Delta G_i^0 - m_i[SDS] \quad (6)$$

where m_i is the slope of free energy change plotted against the denaturant concentration assuming a linear relationship.

By combining eqs 4−6:

$$Y = \{Y_N + Y_{I1}\exp^{-A} + Y_{I2}\exp^{-B} + Y_{I3}\exp^{-C} + Y_U\exp^{-D}\} / \{1 + \exp^{-A} + \exp^{-B} + \exp^{-C} + \exp^{-D}\} \quad (7)$$

where

$$A = \{\Delta G_1^0 - m_i[SDS]\}/RT$$

$$B = \{\Delta G_1^0 + \Delta G_2^0 - (m_1 + m_2)[SDS]\}/RT$$

$$C = \{\Delta G_1^0 + \Delta G_2^0 + \Delta G_3^0 - (m_1 + m_2 + m_3)[SDS]\}/RT$$

$$D = \{\Delta G_1^0 + \Delta G_2^0 + \Delta G_3^0 + \Delta G_4^0 - (m_1 + m_2 + m_3 + m_4)[SDS]\}/RT$$

Equation 7 was used to fit the denaturant-induced unfolding transitions obtained from the fluorescence and absorbance changes and global fitting of both. All of the data were fitted using Sigmaplot 11.

2.5. Electrostatic Potential Calculation. Electrostatic surface potential map of the protein was constructed with Pyton Molecular Viewer of MGL tools, which uses the Adaptive Poisson−Boltzmann Solver (ABPS)[50] to calculate the electrostatic properties. Default parameters were used for the calculations. The input file was prepared from PDB2PQR web server[51,52] using RNase A crystal structure, 1fs3 from the protein data bank. PROPKA[53] was used to assign the protonation states at pH 7.5.

3. RESULTS

3.1. Tyrosine Spectral Changes in SDS. Because the structural changes in RNase A were followed by tyrosine spectral changes, it is necessary to understand the change in absorbance and fluorescence properties of free tyrosine as a function of SDS concentration at similar conditions. The absorbance maximum of tyrosine does not show any considerable shift as increasing the concentration of the surfactant: it stays at 278 nm. However, the absorption coefficient (ε) of tyrosine is altered with SDS concentration, particularly above 0.08 mM. Above this concentration, there is a gradual decrease in the ε value, which increases after 0.6 mM. Similarly, fluorescence emission intensity at 306 nm also shows a turnover at 0.08 mM, which is followed by an increase in fluorescence above 2 mM of SDS. There is a considerable loss of fluorescence above 6 mM. These changes are shown in Figure 2. However, there is no shift in the emission wavelength maximum (Figure S1 in the Supporting Information).

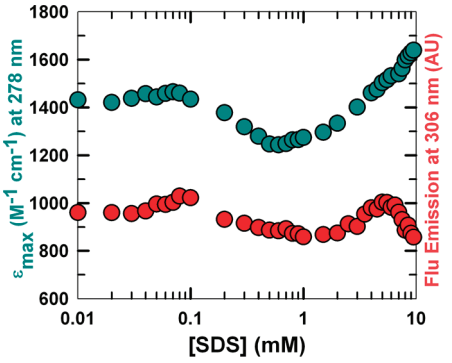

Figure 2. Molar extinction coefficient at 278 nm (blue) and fluorescence emission intensity at 306 nm, after exciting at 280 nm (red), of free tyrosine in varying concentrations of SDS.

Overall, at lower SDS concentrations, no appreciable change in the spectra of tyrosine is observed. When the concentration of SDS increases above 0.1 mM, variations occur both in the absorbance and in the fluorescence of tyrosine. Nevertheless, as compared to the spectral changes of tyrosine residues in RNase A, these changes are less. Therefore, the observed changes in absorbance and fluorescence spectra of tyrosine residues in RNase A are considered to be induced by the conformational changes occur in the protein during denaturation rather than the direct interaction between SDS and tyrosine.

3.2. Fluorescence Studies. RNase A has six tyrosine residues all along its polypeptide chain. Among the six, Y76 is almost completely exposed, Y92 and Y115 are partially exposed, and Y25, Y73, and Y97 are buried inside.[54] Therefore, it is very complicated to deconvolute the contribution of each residue from the total fluorescence intensity of the protein. It has been shown that the fluorescence quantum yield of the protein increases upon denaturation, because of the exposure of buried tyrosine residues.[55] Thus, the total fluorescence intensity change of tyrosine residues can provide a description on global changes in the protein. It has been well studied that tyrosine emission maximum is generally unaffected by local environment changes in RNase A.[42] To confirm the fact that tyrosine does not show any shift in the emission wavelength maximum in the presence of SDS as well, the average emission wavelength maximum[56] was calculated at each SDS concentration from the intensity weighed average of the wavelength between 290 and 320 nm. The plot (Figure S2 in the Supporting Information) clearly evidences that there is no significant change in the emission maximum of tyrosine residues in RNase A upon denaturation and it is constant nearly at 306 nm. Figure 3b presents the change in fluorescence intensity of RNase A as a function of SDS concentration. The transition does not show a simple linear or a sigmoidal change. At least four different transitions were observed when the SDS concentration increases from 0.01 to 8 mM. These transitions were assumed to be due to the formation of three distinct conformational states between the native and the unfolded state. Therefore, the data were fitted into a five-state protein unfolding model using eq 7, and the resultant parameters are given in Table 1.

Mean anisotropy of the tyrosine residues was measured in different SDS solutions at the emission maxima. The results exhibit (Figure 3c) a simple cooperative decrease in anisotropy from 0.8 mM of SDS. Above 4 mM of SDS, there is no considerable change in anisotropy.

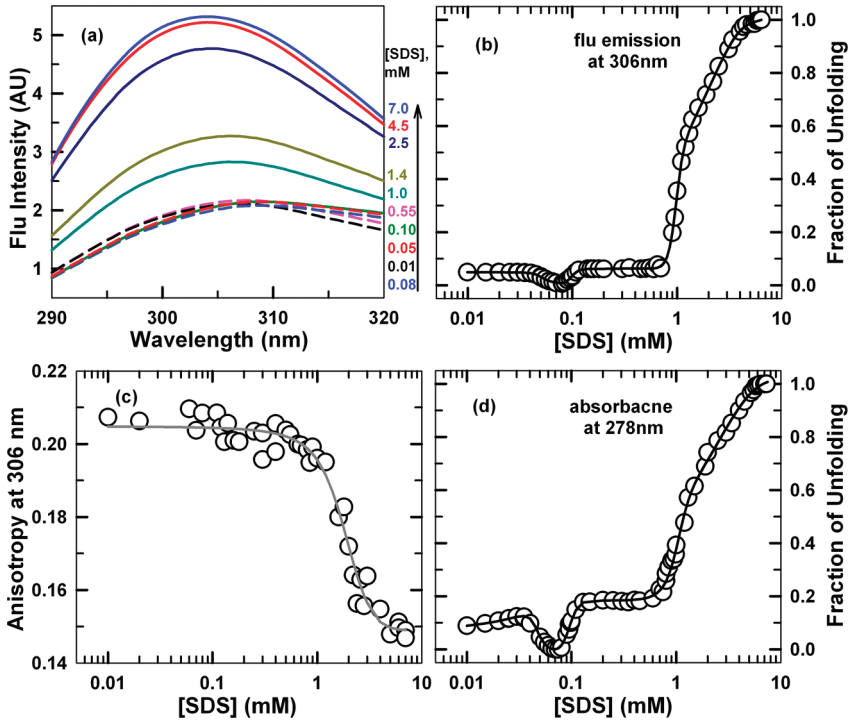

Figure 3. (a) Fluorescence emission spectra of RNase A, excited at 280 nm in varying concentrations of SDS in 20 mM phosphate buffer at pH 7.5. Spectra corresponding to SDS concentrations below 0.6 mM are shown as dotted lines. (b) Fraction of unfolded protein as a function of SDS concentration obtained from fluorescence intensity change at 306 nm. The solid line represents the data fitted into a five-state model using eq 7. (c) Mean anisotropy change of six tyrosine residues of RNase A upon denaturation with SDS. Anisotropy was measured at 306 nm after exciting with polarized light at 280 nm. The solid line is for visual convenience to understand the change. (d) Fraction of unfolded protein as a function of SDS concentration followed by absorption change at 278 nm. For the normalization procedure, see section 3.3. The solid line represents the data fitted into a five-state model using eq 7. Resultant values of the curve fit for (b) and (d) are given in Table 1.

Table 1. Fit Parameters of RNase A Unfolding Transitions in SDS[a]

	region I				region II			
	transition 1		transition 2		transition 3		transition 4	
probe/method	ΔG_1[b]	m_1[c]	ΔG_2	m_2	ΔG_3	m_3	ΔG_4	m_4
fluorescence	6.6	135.9	6.9	73.5	6.5	7.0	0.63	0.27
absorbance	6.5	144.9	5.4	59.4	3.8	3.6	1.0	0.34
global fit	6.0	129.3	6.2	68.5	4.9	4.8	0.60	0.25

[a] All of the transitions were fitted into a five-state model using eq 7. [b] ΔG values are given in kcal mol^{-1}. [c] The m-values are given in kcal mol^{-1} mM^{-1}.

3.3. Absorbance Studies. Change in the extinction coefficient value (ε_{max}) of RNase A at 278 nm shows four distinct transitions similar to the fluorescence studies (Figure S3 in the Supporting Information). However, the transition is more complex than the fluorescence data. To derive more accurate parameters from the available data, the absorbance changes were normalized between the native and unfolded state. To achieve this, the last transition in the absorbance plot where ε_{max} value decreases was considered as the effect of unfolding in the micellar environment, and the fraction of unfolding at 2 mM of SDS was assumed to be equivalent to the amount of unfolding obtained from the fluorescence change, that is, ~75% of denaturation. The resultant normalized curve is shown in Figure 3d.

3.4. Global Fitting. Both the absorbance and the fluorescence data follow the changes around tyrosine residues, and they show a similar trend in the unfolding transitions. Therefore, these two transition curves were fitted globally to obtain the parameters for overall conformational changes occur in the protein while unfolding with SDS (Figure 4). Global fit parameters for eq 7 are shown in Table 1. Within error, the resultant values for all of the parameters are the same as compared to individual fits using the same model.

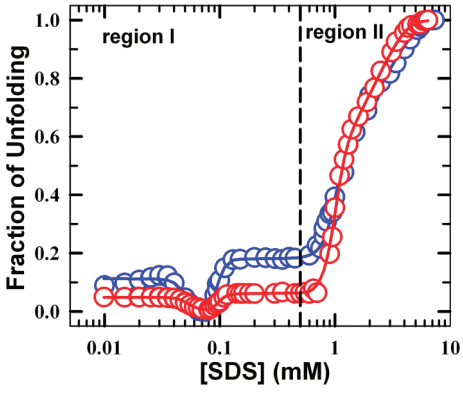

Figure 4. Global fitting of fraction of unfolding data derived from the absorbance (blue) and the fluorescence (red) changes into the five-state model. Solid lines represent simultaneous fit values for both transitions. The parameters obtained from the global fit are given in Table 1. A representative vertical line is drawn to explain two distinct regions, classified on the basis of the RNase A−SDS interaction. For further details, refer to the text.

dx.doi.org/10.1021/jp2062496 |J. Phys. Chem. B 2011, 115, 14760–14767

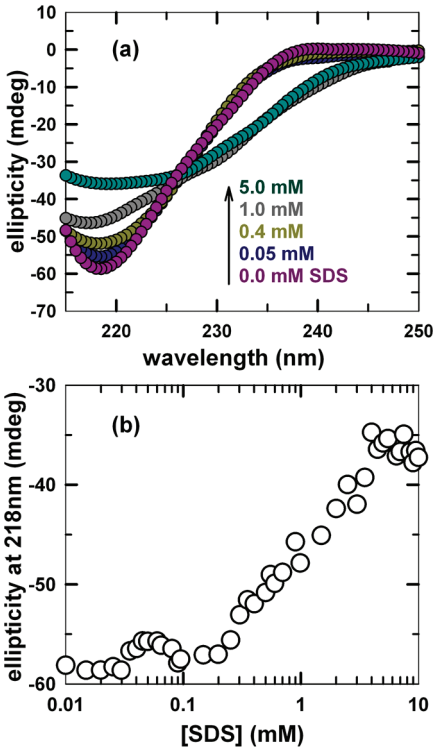

Figure 5. (a) Far-UV CD spectra of RNase A in different concentrations of SDS in 20 mM phosphate buffer, pH 7.5. (b) Change in ellipticity of the protein followed at 218 nm with increasing SDS concentration.

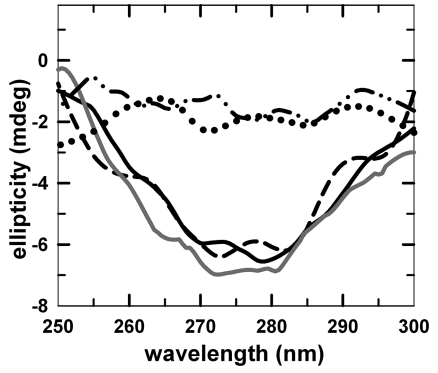

Figure 6. Tertiary structural change of the protein monitored by near-UV CD spectrum. The spectra of RNase A in 0 mM (solid gray line), 0.1 mM (solid black line), 1 mM (dashed line), 2 mM (dotted and dashed line), and 5 mM (dotted line) of SDS are shown.

3.5. Circular Dichroism. The secondary and tertiary structural changes were probed with ellipticity changes of the protein at far- and near-UV regions. From Figure 5, it is evident that increasing SDS concentration reduces the secondary structure content of RNase A. Almost 40−50% of the secondary structure is lost at the highest concentration of SDS used as compared to the native protein. The tertiary interactions are however completely lost at about 2 mM of SDS (Figure 6).

3.6. TNS Fluorescence Probe. TNS is used to investigate protein hydrophobic surfaces.[18] Generally, this organic dye has less fluorescence in water. When it binds to a hydrophobic surface, its fluorescence quantum yield increases even up to 50-fold,

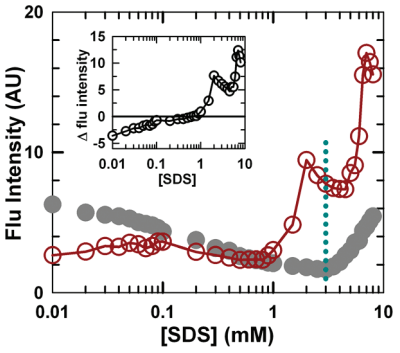

Figure 7. TNS fluorescence emission with increasing concentration of SDS in 20 mM phosphate, pH 7.5 monitored at 440 nm after exciting at 320 nm with (red) and without (gray) RNase A. The dotted vertical line represents the CMC of SDS in the given buffer condition. Inset shows the difference in intensity of TNS emission between the samples with and without protein.

depending on the protein and its conformational state and the polarity of solvent.[57,58] Because SDS also has a hydrophobic tail, the fluorescence of the dye could be altered by varying the concentration of SDS. Therefore, TNS fluorescence was first probed in different SDS concentration solutions as a control. The changes were then measured after adding the protein into the solutions. To simplify the interpretation, the intensity difference between the samples with and without RNase A was plotted against SDS concentration along with the actual fluorescence data (Figure 7 and inset). It is evident from the graph that there was a huge change in fluorescence intensity, when the protein was added, particularly at higher SDS concentrations. It can be attributed to the accessibility of protein hydrophobic surfaces to the dye molecules due to unfolding.

4. DISCUSSION

4.1. CMC of SDS. In the buffer condition adapted for the experiments, SDS shows the CMC value of 3.0 mM, in the absence of protein. It was measured with SO, a fluorescent dye (Figure S4 in the Supporting Information). When the surfactant molecules aggregate to form micelles, the fluorescence intensity of SO increases steeply. The intersection between two transition regions corresponds to the CMC of the surfactant. TNS also can be used as a fluorescent probe to calculate the CMC, which demonstrates the same value (Figure 7).

4.2. Two Regions of Unfolding. On the basis of the results from different probes, the protein unfolding transitions can be divided into two different regions (Figure 4) according to the interaction and major forms of SDS in solution. The region well below the CMC, that is, up to 0.5 mM, involves binding of SDS monomers to the protein. The region around the CMC involves formation of small micellar aggregates to complete micelle formation around the protein. Free energy changes and *m*-values of each transition in both regions were calculated from the fluorescence and the absorbance measurements. To understand the overall effect of SDS binding to the protein, these two spectral probes were fitted globally. All of the resultant parameters are presented in Table 1.

4.3. Region I − Up to 0.5 mM of SDS. The fluorescence and absorbance changes of RNase A clearly demonstrate the presence of at least two different transitions in this region. Region I shows higher free energy changes as compared to the other transitions

occurring in region II (Table 1). In this concentration range, SDS predominantly exists as monomers. Thus, these conformational changes might be attributed to the binding of SDS monomers to specific sites on the protein. From the spectral probes, it can be presumed that there are at least two different kinds of binding steps that occur sequentially in RNase A. In other proteins, the initial monomer binding has been generally found as a single-step cooperative reaction at this concentration range.[13,16] However, in RNase A, the spectral probes suggest two different interaction states for binding. We have here assumed that the conformational changes acquired by the binding of SDS (at ∼0.08 mM concentration) lead to an intermediate state I_1, which further transforms into I_2 upon occupation of additional binding sites by increasing SDS concentration up to 0.5 mM. However, the free energy changes of formation of both of the states are almost the same. This suggests that both the binding sites and the binding interactions are similar in nature. These binding reactions must be induced by the protein surface charges. RNase A has 10 lysine residues, which are positively charged at pH 7.5. They can electrostatically interact with the charged headgroup of the anionic surfactant. These residues are located on the surface, and the binding might not require much unfolding of the protein hydrophobic core. Electrostatic surface potential calculation also supports that RNase A has surface accessible positive charges (Figure S5 in the Supporting Information), and the region specifically between helix 2 and sheet 1 has the highest positive charge on the surface. This region of the protein includes three lysine residues K31, K37, and K41 with a small cleft and a considerable amount of hydrophobic patches nearby, which could facilitate the binding. This region might be the entry point for the following events and responsible for the first transition. There are three tyrosine residues close to this region, Y25, Y92, and Y97. The binding of SDS can alter their conformation, which can be clearly seen from the fluorescence and absorbance changes (Figure 4). The binding of SDS anions at the other parts of the protein surface may be responsible for the second transition monitored by the tyrosine spectral changes. Most of the interactions could happen around the surface where lysine and arginine residues are found in the protein. Although protein unfolding induced by surfactant molecules can be attributed either to ionic or to hydrophobic interactions between them, in the RNase A−SDS interaction we emphasis that at lower concentrations of SDS electrostatic interaction plays a major role. Studies on RNase A activity in the presence of ionic surfactants also predict that the increase in activity is due to ionic interactions, at lower concentrations of SDS.[15−17] In some other proteins[27,34,35] as well, the initial electrostatic binding states have been characterized and considered as a separate intermediate state during unfolding. The importance of these interactions on initializing conformational changes have been well characterized for a β-sheet protein.[20] Moreover, microcalorimetric experiments carried out on different proteins[10,11,14] for the binding of SDS invariably show an exothermic protein−surfactant interaction process, which can also be attributed to the ionic interactions between protein and SDS at lower concentrations. At the same time, there is enough evidence favoring the contribution of hydrophobic interactions at the initial stages of unfolding.[22,23] Therefore, it may be in general concluded that the predominating interaction during protein unfolding by surfactant is determined by the nature of protein and solvent conditions.

In RNase A, at the concentration range of SDS where the monomeric form prevails in the system, most of the secondary and tertiary structures are not altered. From the circular dichroism experiments (Figures 5 and 6), it is evident that the change in secondary and tertiary structure is insignificant (nearly 5%). In many other proteins[13,14] as well, less structural loss at lower concentrations of SDS has been detected, similar to RNase A. Although different transitions are observed with respect to the fluorescence intensity, the mean anisotropy of six tyrosine residues does not change considerably up to 0.8 mM of SDS concentration (Figure 3c). It suggests that the interaction between the solvent and tyrosine residues or the solvent exposure of tyrosine residues is not much altered, whereas small conformational changes arise from the binding of SDS changes the fluorescence intensity. Most of these conformational changes might arise from the breaking of a few tertiary contacts by SDS monomers. It is further confirmed with the fluorescence changes of the hydrophobic probe TNS (Figure 7). TNS fluorescence does not show any increase until 0.8 mM of SDS; in fact, there is a little loss of fluorescence at the lower concentrations from 10 to 80 μM. These results suggest that the initial binding of SDS to RNase A is induced by the positively charged surface residues and modifies the conformations of nearby residues, including tyrosine, without affecting the protein interior.

4.4. High Equilibrium *m*-Value. Generally, for protein unfolding reactions induced by chemical denaturants such as guanidine hydrochloride (Gdn) and urea, *m*-values are less as compared to surfactant-induced denaturation.[15−17] In case of RNase A, urea and Gdn denaturation transitions show 2.75 and 2.99 kcal mol^{-1} M^{-1}, respectively.[55,59] In SDS-induced denaturation, *m*-values are ∼130 and ∼69 kcal mol^{-1} mM^{-1} for the first two transitions, respectively. The *m*-value is the slope of free energy change drawn against denaturant concentration. It reflects the ability of a denaturant to interact with a protein and to effectively change its conformation to another conformational state or to the unfolded state. Therefore, the very high *m*-value for SDS-induced denaturation could be attributed to the fact that the surfactant needs almost 1000 times less concentration to perturb the native conformation of the protein as compared to the other chemical denaturants. At very low concentrations such as 10 mM, the chemical denaturants like urea and Gdn do not show any significant conformational change in the protein. It further emphasizes that the mechanism of unfolding of proteins by surfactants is entirely different from the other chemical denaturants-induced effects.

4.5. Region II − Above 0.5 mM of SDS. In this region, the fluorescence and absorbance show two distinct cooperative transitions approximately from 0.6 to 2 mM and above 2 mM. The transitions III and IV are assumed to be I_2 to I_3 and I_3 to U, respectively. They exhibit relatively low free energy changes and less *m*-values (Table 1). The CD experiments demonstrate that in this region the secondary structure of the protein is significantly affected. At the highest SDS concentration used, the protein loses almost 40−50% of its secondary structure.

The TNS fluorescence probe shows at least three different transitions in this region. When RNase A was added into the solutions containing TNS in varying SDS concentrations, fluorescence started to increase approximately from 1 mM of SDS concentration. It is far less than the CMC of the surfactant in the buffer condition being used. The increase in intensity is due to the unfolding effect induced by SDS on RNase A. As a result, the protein hydrophobic surfaces are exposed and become accessible

to the hydrophobic fluorescent dye. In this region, cobinding of SDS and TNS occurs by hydrophobic interactions with the protein. Because TNS fluorescence is sensitive to hydrophobic interactions, this effect can lead to the increase in its fluorescence emission at lower concentrations of SDS. In this concentration range, binding may arise from the formation of small aggregates of SDS around the protein. SO and TNS fluorescence studies show that the CMC value of SDS is 3.0 mM in the buffer. However, SDS can form small micellar like aggregates even below the CMC induced by the hydrophobic residues of the polypeptide chain. The formation of such aggregates around a protein at lower concentrations of ionic surfactants has been identified in other proteins as well.[28,35]

Fluorescence intensity of TNS starts to decrease considerably between 2 and 4 mM of SDS. Increasing the concentration of SDS above 2 mM could replace the weakly bound TNS molecules from the protein. They are consequently released into a relatively polar solvent environment that quenches their fluorescence. This effect has been noted for acyl-coenzyme-A-binding protein[14] (using ANS, another similar fluorescence probe) and bovine serum albumin[18] as well. The overall free energy change in region II is 6.0 ($\pm$1.0) kcal mol^{-1}. This free energy corresponding to the protein conformational change from the I_2 to U state via I_3 is dominated by hydrophobic interactions between RNase A and SDS. The two distinct transitions (III and IV) in this region may appear due to the different levels of interactions of SDS on the protein. Transition III involves a major free energy change. It may arise from the initial micelle aggregation around the protein hydrophobic sites that breaks the secondary structure. In this transition, the protein loses approximately 30% of its secondary structure. The tertiary structures are also parallelly affected, and at 2 mM SDS they are completely lost (Figure 6). This involves the major denaturation process. Further increase in SDS concentration also disrupts the secondary structure of the protein, and little additional unfolding occurs. As expected, this transition has less free energy change due to the less structural changes occur in the protein. Moreover, this transition corresponding to a lower *m*-value also means that the protein denaturation effect of SDS is less as compared to the lower concentration region (transition III). Transition IV might arise due to the increase of aggregation number of already formed micelle aggregates around the protein, and thus does not incur much unfolding of the polypeptide chain. Experiments on the other protein−SDS complexes have demonstrated that the aggregation number of micelles around the proteins increases with increasing SDS concentration and the size of the micelles formed around the proteins is smaller than the free micelles.[18,38]

A small extent of unfolding detected from the CD and the loss in TNS fluorescence suggest that the higher SDS concentration may induce formation of a few more micelle aggregates. It might occupy the hydrophobic sites available for TNS and releases it into the solvent. It incidentally shows a transition midpoint (2.6 $\pm$ 0.3 mM) around the CMC of SDS. Increasing SDS concentration above 5 mM does not show much change in the fluorescence, and absorbance values predict that most of the unfolding events occur only below this concentration of the surfactant. Yet TNS fluorescence intensity increases sharply above 4.5 mM, probably due to the availability of free SDS micelles. Interestingly, the anisotropy of tyrosine residues decreases in this region, from 1 to 4 mM of SDS, followed by a plateau. It conveys that the tyrosine residues become flexible and the rotational diffusion of these residues increases due to the unfolding of polypeptide chain.[49] It also supports the fact that the major unfolding events occur in this concentration range of SDS.

4.6. Protein−Surfactant Complex Model. Protein denaturation by surfactants has been illustrated using different models.[34,35,43,44] However, the necklace and beads model explains these interactions more satisfactorily than any other model and has much experimental evidence to support it.[18,23,45,46] According to this model, a small clusters of micelles are formed around the protein stabilized by hydrophobic interactions. Two different protein−surfactant complex structures[18] have been proposed by this model: protein wrapping around the micelles and the micelles nucleate at the hydrophobic sites of protein. Our foresaid results can be conveniently explained by the latter model. At lower concentrations, in this case above 1 mM of SDS, micelles are formed around RNase A hydrophobic sites that result in the major unfolding transition. The further increase in concentration might increase the aggregation number and induce formation of a few more micelle structures around the protein. From the five-state unfolding model, we could predict the free energy of formation of the necklace and beads-like structure for the RNase−SDS system that is 5.2 ($\pm$1.0) kcal mol^{-1} (from transition III).

4.7. Comparison with Molten Globule State. Among the three intermediate structures, the first two intermediates I_1 and I_2 closely resemble the molten globule (MG) structure. As a classical description for MG state elucidates, proteins retain most of their secondary structure but lose their tertiary structure contacts at this conformational state.[60] I_1 and I_2, which are formed below 0.6 mM SDS concentration, carry almost all of the secondary and tertiary interactions with little conformational modifications due to SDS binding. Therefore, these states can be assumed to have molten globule-like characters. In fact, SDS has already been shown to induce MG-like structures in globular proteins at different conditions.[12,47,48] The denatured states of RNase A at higher SDS concentrations (around 2 and 5 mM) do lose some of the secondary structure also and do not show a cooperative thermal denaturation (data not shown). Therefore, they cannot be considered as MG states. However, more detailed experimental studies will be carried out in this direction.

5. CONCLUDING REMARKS

SDS-induced unfolding of RNase A was probed using different spectroscopic techniques. The unfolding transitions fit well into the five-state model, assuming formation of at least three intermediate states. The first two transitions, defined as region I, arise from two different kinds of binding sites available for SDS on RNase A surface, and the binding is induced by ionic interactions. It does not considerably affect the protein secondary and tertiary structures. Region II, at higher concentrations of SDS, shows two distinguishable transitions. Hydrophobic interactions predominate in this region, and the exposure of buried residues of the protein to solvent leads to unfolding. SDS monomers form small aggregates on the protein, and specific hydrophobic regions on the protein act as nucleation sites for the aggregation. It appears well below the CMC of SDS. These changes result in the loss of a significant amount of secondary structure content of RNase A, and the tertiary structure is simultaneously completely lost. Increasing the concentration of SDS above 5 mM does not show any significant structural changes.

■ ASSOCIATED CONTENT

Supporting Information. Fluorescence spectra of tyrosine, plots of emission wavelength maximum of RNase A, absorption coefficient of RNase A, and SO fluorescence emission intensity in varying concentrations of SDS, as well as the electrostatic potential map of RNase A. This material is available free of charge via the Internet at http://pubs.acs.org.

■ AUTHOR INFORMATION

Corresponding Author

*Phone: +91 40 2301 3405. Mobile: +91 94930 13047. Fax: +91 40 2301 0120. E-mail: nppsl@uohyd.ernet.in.

Present Address

†Department of Microbiology and Cell Biology, Indian Institute of Science, Bangalore 560 012, India

■ ACKNOWLEDGMENT

This project was supported by DBT, India and a DST-PURSE grant to the University of Hyderabad.

■ REFERENCES

(1) Tadros, T. F. *Applied Surfactants*; Wiley-VCH: Weinheim, 2005.
(2) Kirk, O.; Borchert, T. V.; Fuglsang, C. C. *Curr. Opin. Biotechnol.* **2002**, *13*, 345–351.
(3) Lee, M.; Dordick, J. S. *Curr. Opin. Biotechnol.* **2002**, *13*, 376–384.
(4) Tanford, C. *The Hydrophobic Effect: Formation of Micelles and Biological Membranes*; John Wiley & Sons: New York, 1973.
(5) Shapiro, A. L.; Vinuela, E.; Maizel, J. V., Jr. *Biochem. Biophys. Res. Commun.* **1967**, *28*, 815–820.
(6) Weber, K.; Osborn, M. *J. Biol. Chem.* **1969**, *244*, 4406–4412.
(7) Duquesne, K.; Sturgis, J. N. *Methods Mol. Biol.* **2010**, *601*, 205–217.
(8) Privé, G. G. *Methods* **2007**, *41*, 388–397.
(9) Garavito, G.; Ferguson-Miller, S. *J. Biol. Chem.* **2001**, *276*, 32403–32406.
(10) Andersen, K. K.; Westh, P.; Otzen, D. E. *Langmuir* **2008**, *24*, 399–407.
(11) Lad, M. D.; Ledger, V. M.; Briggs, B.; Green, R. J.; Frazier, R. A. *Langmuir* **2003**, *19*, 5098–5103.
(12) Schneider, G. G.; Shaw, B. F.; Lee, A.; Carillho, E.; Whitesides, G. M. *J. Am. Chem. Soc.* **2008**, *130*, 17384–17393.
(13) Anand, U.; Jash, C.; Mukherjee, S. *J. Phys. Chem. B* **2010**, *114*, 15839–15845.
(14) Andersen, K. K.; Oliveira, C. L.; Larsen, K. M.; Poulsen, F. M.; Callisen, T. H.; Westh, P.; Pedersen, J. S.; Otzen, D. E. *J. Mol. Biol.* **2009**, *391*, 207–226.
(15) Mikšovská, J.; Yom, J.; Diamond, B.; Larsen, R. W. *Biomacromolecules* **2006**, *7*, 476–482.
(16) Chamani, J.; Moosavi-Movahedi, A. A.; Rajabi, O.; Gharanfoli, M.; Momen-Heravi, M.; Hakimelahi, G. H.; Neamati-Baghsiah, A.; Varasteh, A. R. *J. Colloid Interface Sci.* **2006**, *293*, 52–60.
(17) Viseu, M. I.; Carvalho, T. I.; Costa, S. M. B. *Biophys. J.* **2004**, *86*, 2392–2402.
(18) Turro, N. J.; Lei, X.-G.; Ananthapadmanaban, K. P.; Aronson, M. *Langmuir* **1995**, *11*, 2525–2533.
(19) Rowshan, H.; Bordbar, A. K.; Moosavi-Movahedi, A. A. *Thermochim. Acta* **1996**, *285*, 221–229.
(20) Nielsen, M. M.; Andersen, K. K.; Westh, P.; Otzen, D. E. *Biophys. J.* **2007**, *92*, 3674–3685.
(21) Tofani, L.; Feis, A.; Snoke, R. E.; Berti, D.; Baglioni, P.; Smulevich, G. *Biophys. J.* **2004**, *87*, 1186–1195.
(22) Wang, G.; Treleaven, W. D.; Cushley, R. J. *Biochim. Biophys. Acta* **1996**, *1301*, 174–184.
(23) Bhuyan, A. K. *Biopolymers* **2009**, *93*, 186–199.
(24) Otzen, D. *Biochim. Biophys. Acta* **2011**, *1814*, 562–591.
(25) Otzen, D. E.; Nesgaard, A. W.; Andersen, K. K.; Hansen, J. H.; Christiansen, G.; Doe, H.; Sehgal, P. *Biochim. Biophys. Acta* **2008**, *1784*, 400–414.
(26) Yamamoto, S.; Hasegawa, K.; Yamaguchi, I.; Tsutsumi, S.; Kardos, J.; Goto, Y.; Gejyo, F.; Naiki, H. *Biochemistry* **2004**, *43*, 11075–11082.
(27) Ryan, T. M.; Griffin, M. D. W.; Teoh, C. L.; Ooi, J.; Howlett, G. J. *J. Mol. Biol.* **2011**, *406*, 416–429.
(28) Singh, R. B.; Mahanta, S.; Guchhait, N. *Chem. Phys. Lett.* **2008**, *463*, 183–188.
(29) Moriyama, Y.; Watanabe, E.; Kobayashi, K.; Harano, H.; Inui, E.; Takeda, K. *J. Phys. Chem. B* **2008**, *112*, 16585–16589.
(30) Jones, M. N.; Skinner, H. A.; Tipping, E.; Wilkinson, A. *Biochem. J.* **1973**, *135*, 231–236.
(31) Blinkhorn, C.; Jones, M. N. *Biochem. J.* **1973**, *135*, 547–549.
(32) Si-Qing, C.; Xian-Gang, F.; Jian-Fang, Y.; Jie-Hua, L. *J. Dispersion Sci. Technol.* **2007**, *28*, 297–300.
(33) Moosavi-Movahedi, A. A.; Gharanfoli, K.; Nazari, K.; Shamshipur, M.; Chamani, J.; Hemmateenejad, B.; Alavi, M.; Shokrollahi, A.; Habibi-Rezaei, M.; Sorenson, C.; Sheibani, N. *Colloids Surf., B* **2005**, *43*, 150–157.
(34) Reynolds, J. A.; Tanford, C. *Proc. Natl. Acad. Sci. U.S.A.* **1970**, *66*, 1002–1007.
(35) Reynolds, J. A.; Tanford, C. *J. Biol. Chem.* **1970**, *245*, 5161–5165.
(36) Putnam, F. W.; Neurath, H. *J. Am. Chem. Soc.* **1944**, *66*, 692–697.
(37) Jones, A. J. S.; Rumsby, M. G. *Biochem. J.* **1978**, *169*, 281–285.
(38) Gangabadage, C. S.; Najda, A.; Bogdan, D.; Wijmenga, S. S.; Tessari, N. *J. Phys. Chem. B* **2008**, *112*, 4242–4245.
(39) Raines, R. T. *Chem. Rev.* **1998**, *98*, 1045–1065.
(40) Anfinsen, C. B. *Science* **1973**, *181*, 223–230.
(41) Neira, J. L.; Rico, M. *Fold. Des.* **1997**, *2*, R1–R11.
(42) Schmid, F. *Protein Folding Handbook*; Wiley-VCH: Weinheim, 2005; Vol. 1, pp 22−44.
(43) Shirahama, K.; Tsujii, K.; Takagi, T. *J. Biochem.* **1974**, *75*, 309–319.
(44) Lundahl, P.; Greijer, E.; Sandberg, M.; Cardell, S.; Eriksson, K. *Biochim. Biophys. Acta* **1986**, *873*, 20–26.
(45) Chen, S.-H.; Teixeria, J. *Phys. Rev. Lett.* **1986**, *57*, 2583–2586.
(46) Samsó, M.; Daban, J.-R.; Hansen, S.; Jones, J. R. *Eur. J. Biochem.* **1995**, *232*, 818–824.
(47) Moosavi-Movahedi, A. A.; Chamani, J.; Goto, Y.; Hakimelahi, G. H. *J. Biochem.* **2003**, *133*, 93–102.
(48) Halskau, Ø.; Underhaug, J.; Frøystein, N. Å.; Martínez, A. *J. Mol. Biol.* **2005**, *349*, 1072–1086.
(49) Lakowicz, J. R. *Principles of Fluorescence Spectroscopy*, 3rd ed.; Springer: New York, 2006.
(50) Baker, N. A.; Sept, D.; Joseph, S.; Holst, M. J.; McCammon, J. A. *Proc. Natl. Acad. Sci. U.S.A.* **2001**, *98*, 10037–10041.
(51) Dolinsky, T. J.; Czodrowski, P.; Li, H.; Nielsen, J. E.; Jensen, J. H.; Klebe, G.; Baker, N. A. *Nucleic Acids Res.* **2007**, *35*, w522–w525.
(52) Dolinsky, T. J.; Nielsen, J. E.; McCammon, J. A.; Baker, N. A. *Nucleic Acids Res.* **2004**, *32*, w665–w667.
(53) Li, H.; Robertson, A. D.; Jensen, J. H. *Proteins* **2005**, *61*, 704–721.
(54) Noronha, M.; Lima, J. C.; Paci, E.; Santos, H.; Macanita, A. L. *Biophys. J.* **2007**, *92*, 4401–4414.
(55) Pace, C. N.; Laurents, D. V.; Thomson, J. A. *Biochemistry* **1990**, *29*, 2564–2572.
(56) Royer, C. A. *Methods Mol. Biol.* **1995**, *40*, 65–89.
(57) Chiang, H.-C.; Lukton, A. *J. Phys. Chem.* **1975**, *79*, 1935–1939.
(58) McClure, W. O.; Edelman, G. M. *Biochemistry* **1966**, *5*, 1908–1919.
(59) Ahmad, F. *J. Biol. Chem.* **1984**, *259*, 4183–4186.
(60) Ptitsyn, O. *Adv. Protein Chem.* **1995**, *47*, 83–229.